



Cite this: *RSC Appl. Polym.*, 2025, **3**, 675

## Hydroxyl-functional acrylic adhesives: leveraging polysilazane chemistry for curing<sup>†</sup>

Amrita Chatterjee, Shashank Jha, Sushmit Sen, Keshav Dev, Chayan Das and Pradip K. Maji

Acrylic-based wood adhesives are widely recognized for their durability, UV resistance, and rapid drying properties, traditionally achieved using isocyanate-based curing systems despite their inherent toxicity. In this study, the potential of polysilazane (PSZ) as an alternative cross-linker for functional acrylic polymers was evaluated, focusing on adhesive properties. The crosslinking interactions between the acrylic polymer and PSZ formed a highly stable Si–O reinforced three-dimensional network, as characterized by analytical techniques and further supported by enhanced thermal stability and adhesive performance. The PSZ-cured acrylic system exhibited a glass transition temperature ( $T_g$ ) increase to 56 °C from 31 °C of the uncrosslinked copolymer. In the tested range of 10–25 wt% of PSZ, the formulation containing 20 wt% PSZ achieved a 97.9% degree of crosslinking. Compared to traditional diisocyanate-crosslinked systems, better adhesive performance was obtained with maximum tensile shear strength values of 4.4 MPa for wood substrates (substrate failure) and up to 4.0 MPa for aluminum substrates. These findings confirm that PSZ enhances the mechanical properties of acrylic adhesives, offering optimal performance and ease of application and underscoring their practical utility.

Received 2nd December 2024,

Accepted 6th March 2025

DOI: 10.1039/d4lp00354c

rsc.li/rscapplpolym

## 1 Introduction

Acrylic adhesives constitute an important class of bonding materials, valued for their excellent wetting characteristics, chemical resistance, high shear strength, and outstanding film-forming capabilities.<sup>1,2</sup> Thermoplastic film adhesives based on acrylates are often formulated by blending alkyl acrylates with acrylonitrile, tailoring their properties through structural modifications and copolymerizing with functional monomers.<sup>3,4</sup> Introducing small amounts of polyfunctional vinyl monomers produces flexible adhesives with enhanced creep resistance, while higher concentrations create rigid, heat- and solvent-resistant three-dimensional thermoset networks. Hydroxyl-functionalized monomers are frequently used to increase the system's polarity and provide reactive sites for cross-linking, facilitating the conversion of the polymer into thermoset adhesives. Cross-linking polyfunctional acrylic

monomers, either during polymerization or post-application, yield high-strength, solvent-resistant adhesives.<sup>5</sup> Heat, high-energy radiation, or cross-linking agents such as polyisocyanates, epoxides, or low-molecular-weight urea, melamine, and phenol-formaldehyde resins can induce this cross-linking process, reacting with functional groups like  $-\text{OH}$ ,  $-\text{NH}_2$ , and  $-\text{COOH}$  in the polymer.<sup>6</sup>

Acrylic adhesives are predominantly cured with isocyanates, which form robust cross-linked networks that significantly enhance mechanical properties such as strength and chemical resistance. These classes of adhesives can also be crosslinked with various crosslinkers<sup>7</sup> to suit specific needs such as poly-functional acrylates like TMPTA (Trimethylolpropane triacrylate) for UV resistance and strength,<sup>8</sup> or epoxy resins to boost chemical and heat resistance,<sup>9</sup> while aziridines ensure quick curing and durability.<sup>10</sup> Recently amino silanes like APTES have been used to promote adhesion to inorganic surfaces.<sup>11</sup> However, concerns regarding the health and environmental risks associated with the leading option isocyanates—such as the release of volatile organic compounds (VOCs) and respiratory hazards—have prompted the search for safer alternatives.<sup>12</sup>

Silicon-based modifications offer an effective strategy to enhance acrylic-based coatings and adhesives, leveraging silicon's inherent flexibility, weather resistance, and thermal stability.<sup>13,14</sup> These enhancements improve resistance to UV radiation and moisture, while also expanding adhesion to non-polar and low-surface-energy substrates.<sup>15</sup> The interaction and

<sup>a</sup>Department of Polymer and Process Engineering, Indian Institute of Technology Roorkee, Saharanpur Campus, Saharanpur 247001, India.

E-mail: pradip@ppe.iitr.ac.in

<sup>b</sup>Department of Chemistry, Visvesvaraya National Institute of Technology, Nagpur, Maharashtra 440010, India

<sup>c</sup>Department of Chemistry, Indian Institute of Technology Roorkee, Roorkee, 247667, India

<sup>†</sup>Electronic supplementary information (ESI) available. See DOI: <https://doi.org/10.1039/d4lp00354c>

<sup>‡</sup>Equal Contributions (These authors have contributed equally to this work).



chemistry of the silane and acrylic components have been described in depth in a work by Andre *et al.*<sup>16</sup> Amino silanes enhance adhesion between acrylate polymers and glass by forming chemical bonds. The silane's methoxy head groups bond with silanols on the glass, leaving amine groups to interact with carboxylic acid functionalities in the polymer, creating ionic bonds. This modification improves interfacial structure, promotes molecular ordering, and strengthens adhesion, making it valuable for applications requiring robust polymer-glass interfaces.<sup>17</sup> In the work of Pan *et al.*, a silicon-based adhesion promoter was synthesized and applied to addition-type silicone rubber, enhancing bonding performance and compatibility. At 2.0 phr, it achieved a shear strength of 1.33 MPa with copper while maintaining ~90% transmittance and improving wettability (contact angle reduced from 52.1° to 48.2°). The modification effectively improved adhesion and preserved optical properties, making it suitable for silicone-modified acrylic adhesives.<sup>18</sup>

Keeping the chemistry and advantages in mind, another material, polysilazanes, characterized by their alternating Si–N backbone units, present a promising alternative to isocyanates for curing acrylic adhesives.<sup>19,20</sup> These compounds react with the hydroxyl (–OH) groups in acrylic polymers, forming a robust three-dimensional network *via* Si–O–Si cross-links.<sup>21</sup> Polysilazane-cured systems offer numerous benefits, including reduced toxicity, lower environmental impact, and enhanced thermal and chemical resistance compared to isocyanate-cured adhesives.<sup>22,23</sup> Their inorganic Si–N structure further enhances stability under extreme conditions, positioning polysilazanes as a viable option for high-performance adhesive formulations.<sup>24</sup> The study by Widystuti *et al.* investigates the effects of particle size, YSZ content, and curing time and temperature on the thermal conductivity and adhesion strength of thermal barrier coatings (TBCs) made from YSZ/polysilazane. Despite their demonstrated utility in coatings, the application of polysilazanes in adhesive systems remains underexplored.<sup>25</sup>

This study investigates the potential of polysilazane as a cross-linking agent for thermoset film adhesives derived from hydroxyl-functional acrylic polymers. Thermal curing was employed to achieve cross-linking, and the resulting adhesive properties, thermal behavior, and cross-link density were systematically analyzed. The adhesives were tested on both wood and metal substrates, chosen for their relevance in industries where strong, durable bonding is required under various environmental conditions providing reliable bonding under varying conditions, such as moisture, temperature fluctuations, and mechanical stress. This exploration aims to establish polysilazane-based acrylic adhesives as an easy-to-apply, high-performance alternative for demanding applications across a range of materials.

## 2 Materials and methods

### 2.1 Materials

Methyl methacrylate (MMA, C<sub>5</sub>H<sub>8</sub>O<sub>2</sub>), Stearyl methacrylate (SMA, C<sub>22</sub>H<sub>42</sub>O<sub>2</sub>), 2-Hydroxy-ethyl acrylate (HEA, C<sub>5</sub>H<sub>8</sub>O<sub>3</sub>),

Butyl acetate (BuAc, C<sub>6</sub>H<sub>12</sub>O<sub>2</sub>), Azo-bis-isobutyronitrile (AIBN, C<sub>8</sub>H<sub>12</sub>N<sub>4</sub>), were purchased from Sigma-Aldrich. Polysilazane grade Durazane 1500 ((CH<sub>3</sub>)<sub>2</sub>Si-NH)<sub>n</sub> slow cure and TDI (Toluene diisocyanate based crosslinker, blocked with pentanedione, deblocking temperature 80–85 °C) were obtained from SBL Specialty Coatings Private Limited, India. The acrylic monomers were used after inhibitor removal. Wood panels were purchased from the local market of Saharanpur, India.

### 2.2 Methods

An acrylic copolymer was synthesized using methyl methacrylate (MMA), stearyl methacrylate (SMA), and 2-hydroxyethyl acrylate (HEA) as monomers, with 2,2'-azobisisobutyronitrile (AIBN) serving as the free radical initiator. The polymerization was carried out *via* solution polymerization in butyl acetate (BA) as the solvent, as illustrated in Fig. 1a.

The selection of monomers was guided by their specific contributions to the copolymer's properties. MMA, with its short chain length, imparts hardness to the resin, while SMA contributes flexibility due to its longer chain length. HEA, a functional monomer, provides plasticity and serves as a cross-linking site for the copolymer. Three initial batches of the copolymer were synthesized, each with a different monomer ratio, as summarized in Fig. 1c. The copolymer with a composition of MMA:SMA:HEA = 40:40:20 wt% exhibited the optimal viscosity for adhesive applications without requiring additional solvent (Fig. 1S†). The polymerizations were conducted in a 500 mL four-necked, jacketed glass reactor equipped with a reflux condenser, an efficient stirrer, a dropping funnel, and a nitrogen inlet. Initially, half the quantity of AIBN and solvent was charged into the reactor and heated to 80 °C. Once the reflux began, the monomer mixture, the remaining solvent, and the initiator solution were gradually added *via* a syringe over two hours while maintaining constant stirring at 80 °C. The reaction proceeded until the viscosity of the mixture increased significantly, indicating polymerization.

Following copolymer formation, a portion of the resin was mixed with a calculated amount of polysilazane as a cross-linker (Table 2). Due to the evolution of ammonia (Fig. 1b), effervescence was observed during the mixing process, suggesting an active reaction between the copolymer and the curing agent. The amine-containing moieties (–NH) and –OH of the copolymer undergo hydrolysis and condensation reaction, releasing ammonia forming the Si–O bonds. After thorough mixing, the adhesive was applied uniformly to the substrate. The coated panels were oven-cured at 80 °C for 1 hour and then allowed to cool to room temperature before undergoing performance testing.

## 3 Characterization

In the Attenuated Total Reflectance (ATR) mode, the chemical structure of the produced resin was examined using an FTIR spectrometer (PerkinElmer FTIR, ATR spectrum Two). Within



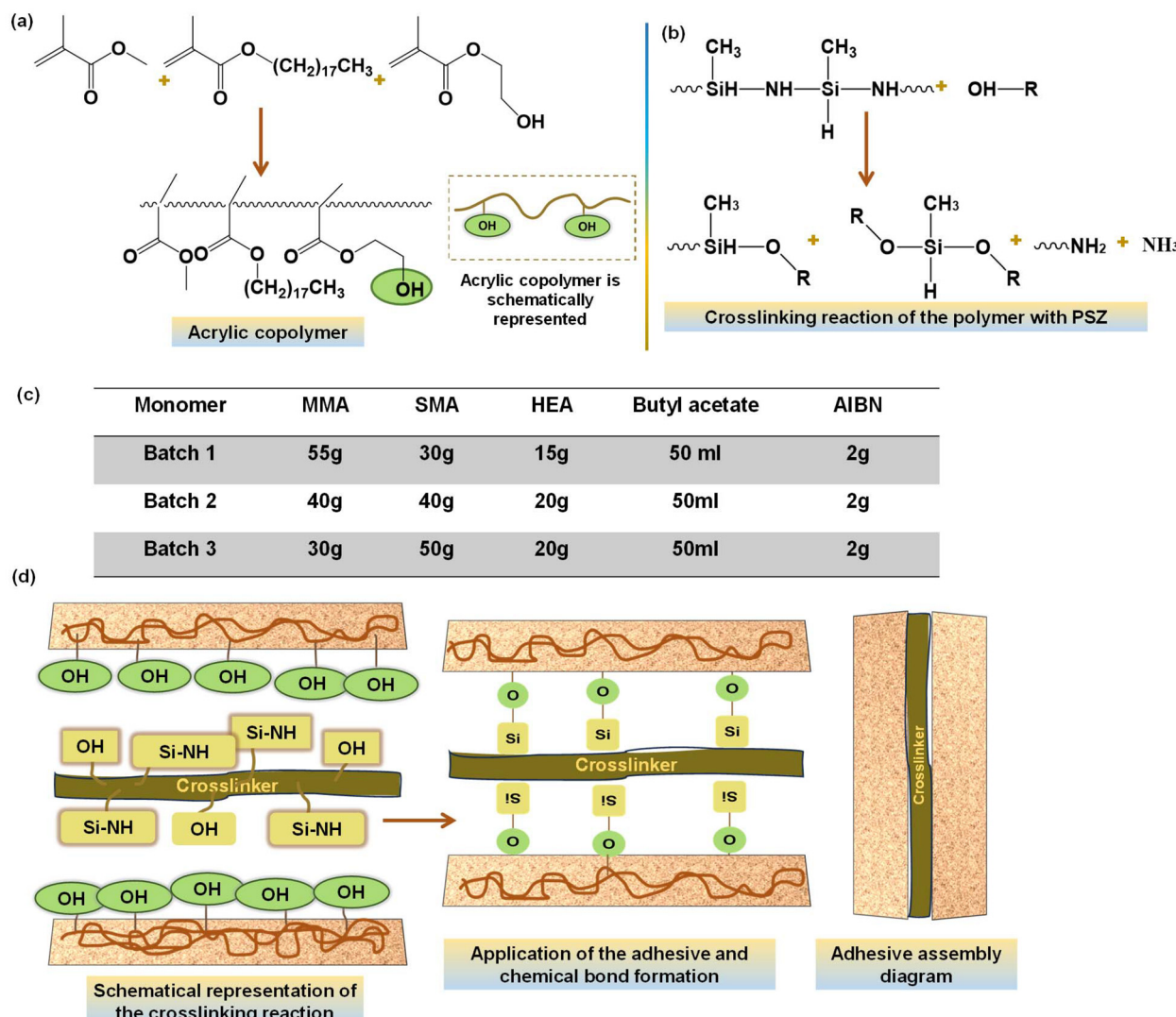


Fig. 1 (a) Copolymer synthesis reaction, (b) Curing reaction of PSZ with Acrylic copolymer, (c) different formulations of the acrylic resin, (d) schematic representation of adhesion curing and adhesive assembly.

the  $400\text{ cm}^{-1}$  to  $4000\text{ cm}^{-1}$  range, the scanning rate was maintained at  $4\text{ cm}^{-1}$ .

The thermal characteristic of the material was examined using a HITACHI TG/DTA 7200 thermogravimeter and differential thermogravimeter. The resins were heated at  $10\text{ }^{\circ}\text{C}$  per minute to a temperature range of  $30\text{ }^{\circ}\text{C}$  to  $600\text{ }^{\circ}\text{C}$  while contained in a Platinum sample pan.

To calculate the molecular weight, 10 mg of polymer sample was placed in a 100 mL glass beaker and 20 ml of tetrahydrofuran was added and stirred for 10 min. To guarantee full dissolution in THF, the samples were held for two to three hours.

Following that, the samples were passed through a  $0.45\text{ }\mu\text{m}$  syringe filter. For analysis,  $50\text{ }\mu\text{L}$  of samples were put into a GPC column.

The solid content of the adhesive was measured using the oven-drying method.<sup>26</sup> About 3 g (initial weight, A) of the

adhesive was placed in an oven and dried at  $105\text{ }^{\circ}\text{C}$  for several hours until a constant weight (B) was achieved. The solid content was then calculated using a specific formula. The average solid content was determined based on three parallel samples.

$$\text{Solid content (wt\%)} = \frac{B}{A} \times 100 \quad (1)$$

The acrylic-PSZ film sample, with a known initial weight, was submerged in methyl ethyl ketone (MEK) for 24 hours. After the immersion period, the sample was removed, dried in an oven until a constant weight was reached, and subsequently used to calculate the gel content of the film, following eqn (2):<sup>27</sup>

$$\text{Gel content (wt\%)} = \frac{W_w}{W_d} \times 100 \quad (2)$$

$W_w$  is the dried film's weight, and  $W_d$  represents the initial weight.

Adhesive samples were heated in an oven at 80 °C until a constant weight ( $W_c$ ) was achieved. The cured adhesives were then immersed in tap water at room temperature for 24 hours, followed by oven-drying at 100 °C for 5 hours until a stable weight ( $W_s$ ) was obtained. The residual rate was calculated as the ratio of  $W_s$  to  $W_c$ , as expressed in eqn (3). The average residual rate was determined using three parallel samples.<sup>26</sup>

$$\text{Residual rate (wt\%)} = W_s/W_c \times 100 \quad (3)$$

The produced films' hardness levels were determined using ASTM D3363. Lead pencils with a wide variety of hardness levels were utilized in this experiment. The reported pencil hardness is the pencil's number that prevents visible scratches from appearing on the film's surface.

Setting time is another important parameter to keep in mind for adhesive's usability. A small amount of glue was placed onto a wood substrate with the use of a thin spatula to calculate the setting time. The spatula was used to pull threads from the resin repeatedly until thread formation became infeasible. The set-in period was considered to have passed when no thread creation was seen.

The tensile shear strength of the adhesives was studied using a universal testing machine. One end of the wood piece was coated with a precisely measured quantity of glue in such a way that the surface was appropriately moistened. After that, the adhesive-coated wood pieces were put together such that their grains ran parallel to one another. Following the clamping time, and drying in an oven at 80 °C for an hour, the panels were cooled down to room temperature, before being taken for testing. The sample was pushed apart at a regulated rate of 10 mm min<sup>-1</sup> while being held by vice grips at each end. The force used was proportionate to the total adhesive surface area.

$$\text{Bonding strength (MPa)} = \frac{\text{tension force (N)}}{\text{gluing area (m}^2\text{)}} \quad (4)$$

## 4 Results and discussion

### 4.1 Characterization of the adhesive formulations

The FTIR spectrum of the synthesized resin sample reveals a broad peak attributed to O-H stretching vibrations in the range of 3412–3460 cm<sup>-1</sup> (Fig. 2). Another prominent broad peak, observed between 2842–3000 cm<sup>-1</sup>, corresponds to the C-H stretching vibrations of methyl and methylene groups. In the spectrum of the acrylic resin, the region between 1600–1800 cm<sup>-1</sup> is indicative of carbonyl (C=O) stretching vibrations. A distinct peak at 2160 cm<sup>-1</sup> originates from the Si-H groups of polysilazane and is present in all cured resin samples.<sup>28</sup> The addition of the curing agent, polysilazane, results in a decrease in the intensity of the hydroxyl group peak, suggesting that the O-H groups have reacted with PSZ. Furthermore, new peaks appear in the range of 1200–940 cm<sup>-1</sup>, corresponding to Si-O lin-

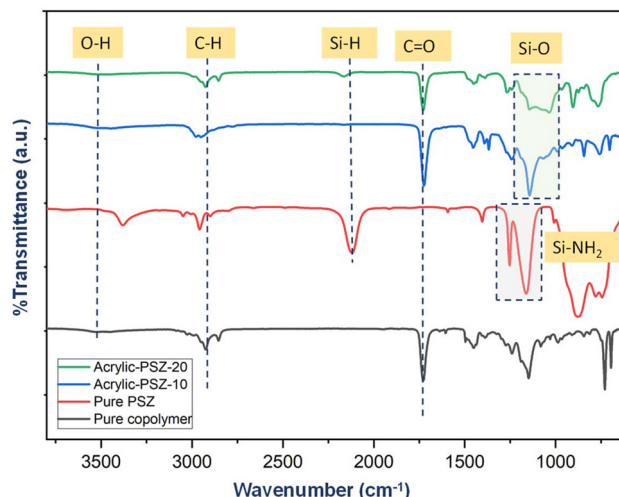


Fig. 2 FTIR spectrum between copolymer and PSZ.

kages formed during cross-linking between polysilazane and the hydroxyl groups of the acrylic resin. These newly developed peaks are particularly evident in the spectra of Acrylic-PSZ-10 and Acrylic-PSZ-20, demonstrating successful cross-linking between the polysilazane and the acrylic resin.<sup>21,29</sup>

### 4.2 Thermal property of the adhesives

Understanding the thermal characteristics of a material is essential, as it provides insight into how the material will behave under varying temperature conditions. The thermal properties of the synthesized copolymer and adhesive formulations are illustrated in Fig. 3. As shown in Fig. 3b, the synthesized copolymer exhibits a glass transition temperature ( $T_g$ ) of around 31 °C. The copolymer displays two transitions: one corresponding to the harder MMA segment and another associated with the more flexible SMA segment. However, during cross-linking, the formation of a dense network causes these distinct segment characteristics to merge, and the material behaves as a unified whole. Consequently, only one  $T_g$  is observed in the cured formulation.<sup>30</sup> With the increased addition of polysilazane (PSZ), the  $T_g$  of the copolymer increases to 56 °C, indicating a higher degree of cross-linking. As the number of chain segments that can independently exhibit transitions at  $T_g$  decreases, more heat is required to achieve the transition, resulting in an elevated  $T_g$ .

Thermal stability was further assessed through thermogravimetric analysis (TGA), as shown in Fig. 3a. The addition of PSZ as a cross-linker significantly enhances the thermal stability of the resin. As observed in the DSC results, thermal stability improves with increasing PSZ content. This improvement is attributed to the higher degree of cross-linking, which results in the formation of a dense three-dimensional network structure, as well as an increase in the silicon content within the system.<sup>24</sup>



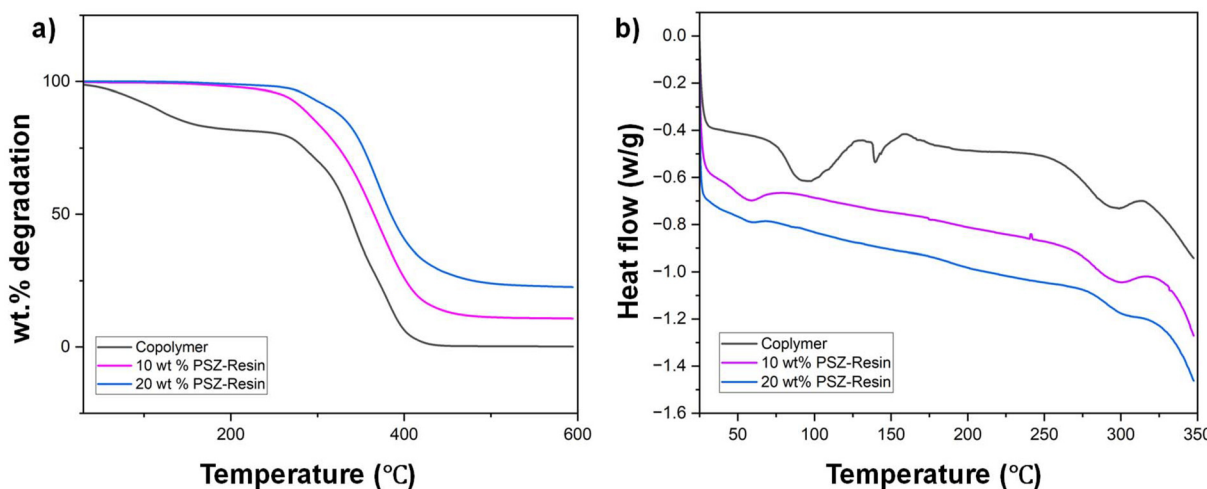


Fig. 3 (a) Thermal stability and (b) thermal transition profile of the polymer.

#### 4.3 Molecular weight analysis of the synthesized polymers

The molecular weight of the synthesized resin with optimal usable viscosity (containing 20 wt% HEA) was determined using gel permeation chromatography (GPC), the result is illustrated below in Fig. 4. The molecular weight ( $M_n$ ) was found to be  $2.428 \times 10^3$  g mol $^{-1}$ , which is considered the optimal molecular weight for the system, providing the optimal viscosity for adhesive applications.<sup>31</sup> The methyl methacrylate (MMA) segments contribute to the increase in viscosity, while the stearyl methacrylate (SMA) segment plays a key role in controlling the flexibility of the polymer. Together, these segments balance the viscosity and flexibility of the polymer, making it suitable for adhesive use. The monomer ratio was carefully selected to maintain the desired viscosity of the polymer. Increasing the proportions of MMA leads to a rapid rise in viscosity, making the adhesive difficult to apply without the addition of external solvents. Conversely, increasing the SMA content improves the tack of the system, but this can also reduce the bond strength of the adhesive.

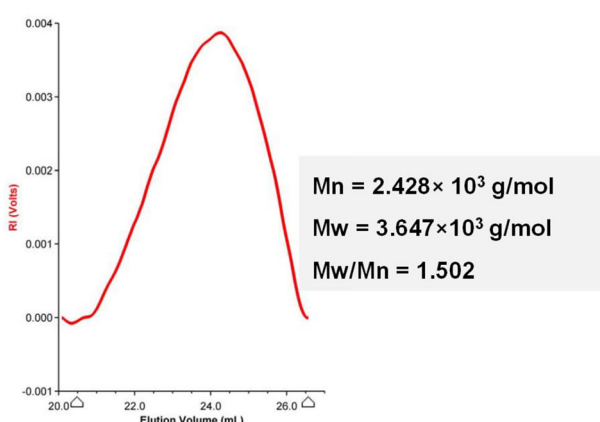


Fig. 4 Determination of molecular weight of the polymer by GPC.

#### 4.4 Solid content, gel content, and residual rate of the adhesives

Solid content significantly affects the performance of wood adhesives, as higher solid content generally improves bonding. Low solid content requires more solvent removal during drying and clamping time, potentially weakening the plywood bond. As shown in Fig. 5, the pure polymer had a solid content of 27.7 wt%, adding polysilazane progressively increased the adhesive's solid content, reaching up to 39.9 wt% for the acryl-PSZ-20 formulation, exhibiting a 30.7% improvement over the pure polymer.

The degree of crosslinking in the cured resin films was assessed using a solvent immersion test, by determining the gel content. A sample of the cured film, with a known initial weight, was immersed in MEK for 24 hours. The resulting swollen gel was then dried at 100 °C, and the weight of the dried film was recorded to determine the weight loss. The acryl-PSZ-10 exhibited a 94.7% degree of crosslinking, while acryl-PSZ-20 demonstrated a higher extent of crosslinking at 97.9%.

Water resistance, measured by the residual rate, is a critical property of wood adhesives. The adhesive had a residual rate of 85.1 wt%, due to the presence of hydrophobic groups. Incorporating polysilazane further enhanced water resistance, with the acryl-PSZ-10 formulation achieving a 91.5 wt% residual rate and acryl-PSZ-20 up to 95.6 wt% due to crosslinking between hydroxyl groups and polysilazanes.<sup>22</sup> Overall, low surface energy and less water absorption also provides longevity of the adhesive system on wood.<sup>32</sup> All the data is represented below in Fig. 5a–c.

#### 4.5 Pencil hardness of the adhesives

The presence of MMA is the key factor that influences the hardness of the film, while SMA and HEA impart flexibility. Without the addition of any crosslinker, the dried copolymer film shows a hardness of 2H.<sup>33</sup> Additionally, the incorporation



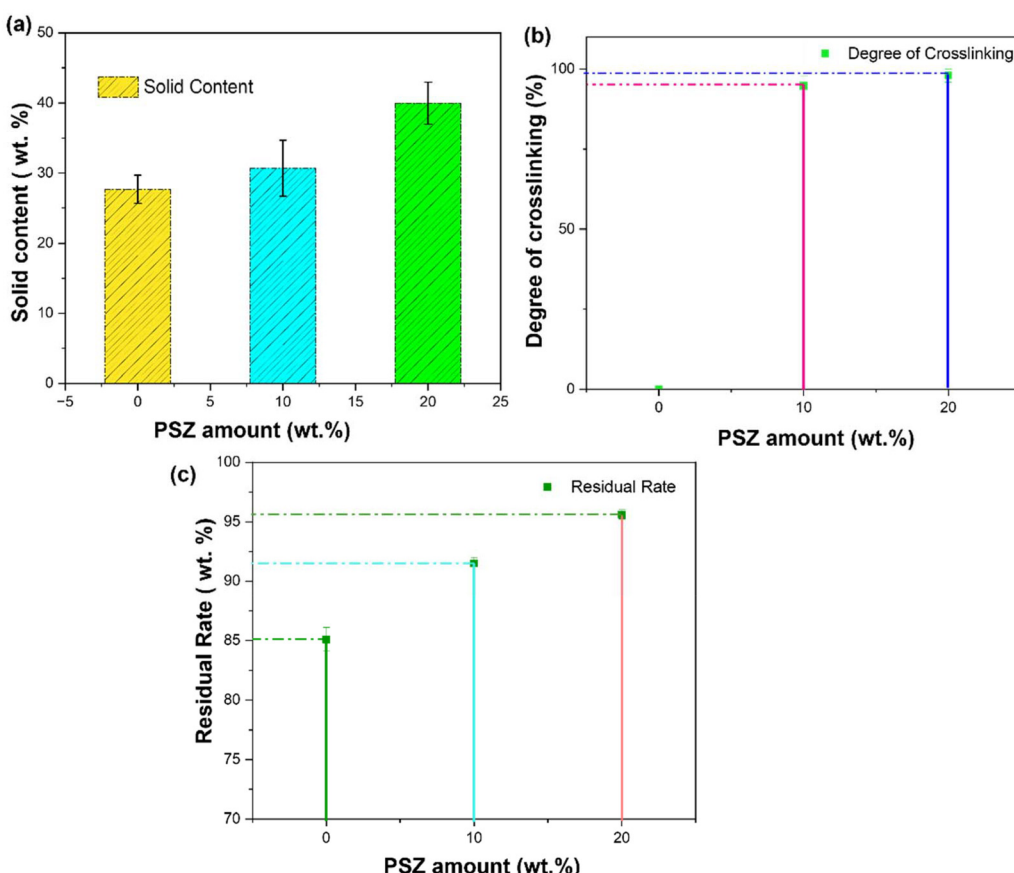


Fig. 5 Change of (a) solid contents, (b) degree of crosslinking, (c) residual rate, with different amounts of crosslinker.

of polysilazane (PSZ) as a cross-linker significantly enhances the hardness of the system, leading to the formation of a densely cross-linked structure. This increased cross-linking results in a more robust cured adhesive, making the surface progressively harder and more resistant to scratching. In this study, after 1 hour of curing, the film hardness was observed to reach 6H, indicating a substantial improvement in surface hardness.<sup>30</sup>

#### 4.6 Setting time of the adhesives

Setting time refers to the duration required for the solvent in the adhesive to fully evaporate. As the solvent evaporates, the adhesive dries and bonds to the substrate. The incorporation of highly reactive polysilazane into the system accelerates this process, reducing the overall setting time.<sup>34</sup> With varying amounts of PSZ, the setting time changed accordingly. Under ambient conditions, the setting time for the adhesive with 10–20 wt% of PSZ is within 45 minutes, indicating a rapid drying and curing process. But around 25 wt% of PSZ, the formulation got gelled with a minute of mixing.

#### 4.7 Morphology of the adhesives

Fig. 6a–d presents surface micrographs of various cured adhesives. The pure acrylic polymer film surface showed a very

wavy-irregular structure, indicative of solvent evaporation during the drying process. When polysilazane was added, the surface became smooth, because of the formation of a cross-linked denser structure. Incorporating more polysilazane further improved the homogeneity of the structure by creating a strong cross-linked network, effectively blocking moisture and enhancing water resistance. However, an excessive amount of polysilazane led to rapid evaporation of ammonia leading to holes and cracks. The surplus polysilazane disrupted the adhesive's structure and promoted a foam-like material (Fig. 6d inset). These observations are accounted for below.

#### 4.8 Tensile shear strength analysis of the adhesives

The tensile shear strength of the adhesives was evaluated using a universal testing machine (UTM) operating at a cross-head speed of 10 mm min<sup>-1</sup>. To ensure consistency and eliminate the influence of bonding area variations on adhesive performance, the application area was standardized at 9 cm<sup>2</sup>. The strength of the adhesive is dependent on the extent of cross-linking between the acrylic polymer and polysilazane.

During the reaction with hydroxyl group of the acrylic, polysilazane (PSZ) chains undergo cleavage of Si–N bonds, resulting in shorter chain lengths and the formation of additional

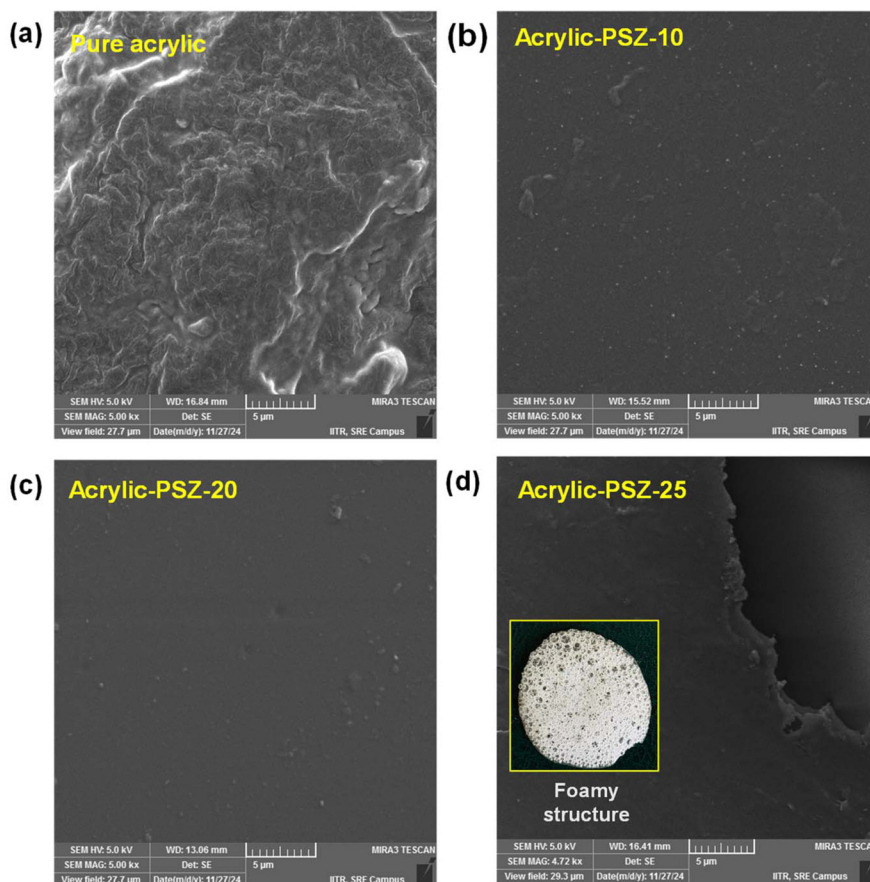


**Fig. 6** SEM micrographs of adhesives with different PSZ concentrations (a) pure acrylic polymer (b) adhesive with 10 wt% of PSZ, (c) adhesive with 20 wt% of PSZ, (d) adhesive with 25 wt% of PSZ, generating a foamy structure, inset picture shows foamy structure formed by reaction with excess PSZ.

Si–O bonds.<sup>35</sup> Cross-linking is primarily attributed to the trifunctional (–Si(H)–NH–) groups in PSZ, which facilitate condensation reactions with alcohol-containing species on hydroxyl-functional polymers. This mechanism highlights a novel application of polysilazanes as curing agents for adhesives.<sup>36</sup> Additionally, the incorporation of silicon into the hybrid network is expected to enhance thermal properties, offering improved performance under challenging conditions. The cross-linking mechanisms are illustrated in Fig. 1b.

To achieve an adequately cured adhesive system, an excess of PSZ—ranging from 20 to 30 wt%—is typically required.<sup>36</sup> In this study, the best performance was observed at 20 wt%. This off-stoichiometric requirement arises from the breakdown of PSZ chains and the concurrent release of ammonia (NH<sub>3</sub>), which hinders the efficient reaction between -OH functional groups and remaining -NH groups.<sup>22</sup>

Despite efforts to optimize the curing process, completely suppressing foaming effects proved challenging, even in dilute PSZ solutions. The use of high concentrations of PSZ inevitably generates significant ammonia gas during decomposition, leading to defects such as bubbles within the adhesive. These bubbles reduce the overall bond strength of the prepared

adhesives, highlighting a trade-off between PSZ concentration and adhesive performance.

The tensile shear strength results, presented in Fig. 7a, b and Tables 1–3, highlight that the optimal adhesive performance was achieved with a resin-to-crosslinker ratio of 3 : 0.6 by weight. While polysilazanes possess a relatively low molecular weight, resulting in a higher weight percentage compared to conventional crosslinkers, this does not imply an excessively high molar quantity of crosslinkers. Attempts to determine the molecular weight of polysilazanes *via* gel permeation chromatography (GPC) were inconclusive; thus, the adhesive formulations were defined based on weight given the novelty of using polysilazanes as crosslinkers, no precedent exists in the literature. Consequently, an iterative experimental approach, inspired by the bisection method in numerical analysis, was adopted. This method commenced with two initial resin-to-crosslinker formulations, followed by iterative refinement. Each subsequent formulation was designed to (a) represent a midpoint between the initial formulations and (b) refine the combination yielding superior tensile shear strength. This iterative process continued until a single formulation consistently demonstrated superior performance over successive iterations.



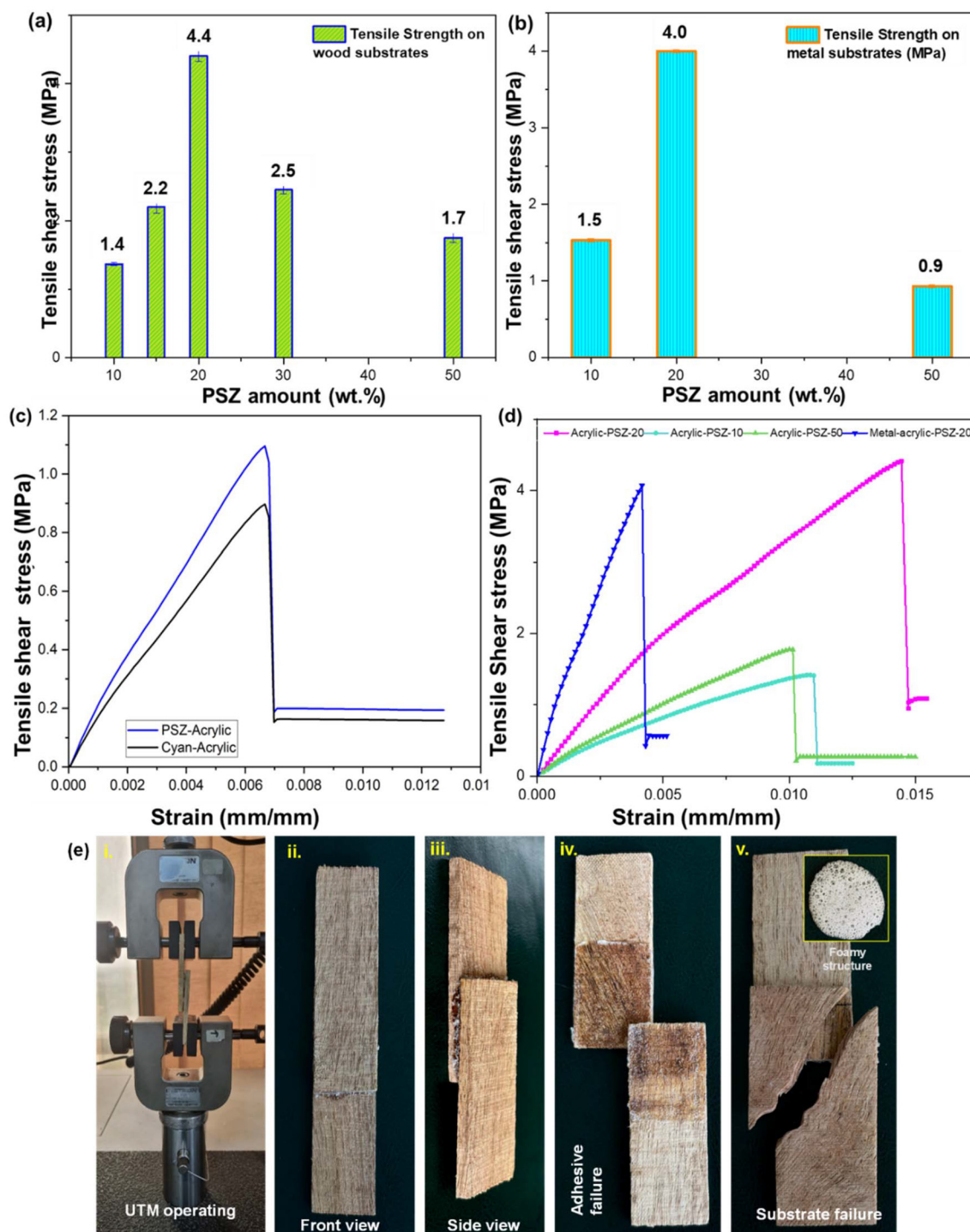


**Fig. 7** (a) Strengths of the polysilazane-cured adhesive formulations with wood substrates, (b) strengths of the polysilazane-cured acrylic adhesive formulations for metal substrates, (c) Tensile shear strengths of acrylic adhesive formulations with conventional crosslinker and PSZ, (d) Tensile shear strengths of adhesives with varying amount of PSZ, (e) UTM operating assembly and substrate pictures, with modes of failure, inset picture with foamy-structure of formulation with excess PSZ.

Inadequate crosslinking, as observed in formulations such as 3 : 0.3 and 3 : 0.5, led to reduced tensile shear strength and adhesive failure (Table 2 and Fig. 7e(iv)). Conversely, excessive polysilazane content, as in the 3 : 1 and 3 : 1.5 formulations,

caused substantial  $\text{NH}_3$  released during curing. This resulted in the formation of a brittle, foam-like structure (Fig. 7e(v), inset picture), compromising adhesive integrity.<sup>36–38</sup> However, the optimal formulation of 3 : 0.6 by weight demonstrated the

**Table 1** Adhesive performance of polysilazane cured resin and conventional diisocyanate cured system (shown in Fig. 7c)

Resin taken (g)	Type of crosslinker used (5 wt% of the resin)	Avg. strength (MPa)
3	TDI based crosslinker	0.9
3	Polysilazane	1.1

**Table 2** Adhesive performance of polysilazane-cured acrylic polymer on wood substrates (shown in Fig. 7d)

Amount of resin (g)	Amount of polysilazane (g)	PSZ amount in wt% of the resin	Strength average (MPa)	Type of failure
3	1.5	50	1.7	Adhesive
3	1	30	2.5	Adhesive
3	<b>0.6</b>	<b>20</b>	<b>4.4</b>	<b>Substrate</b>
3	0.5	16	2.2	Adhesive
3	0.3	10	1.4	Adhesive

**Table 3** Adhesive performance of polysilazane-cured acrylic polymer on wood substrates (shown in Fig. 7d)

Amount of Resin (g)	Amount of polysilazane (g)	Avg. Strength (MPa)
3	0.3	1.5
3	0.6	<b>4.0</b>
3	1.5	0.9

highest tensile shear strength, leading to substrate failure rather than adhesive failure (Fig. 7e(v)). At this ratio, polysilazanes formed a robust, dense network with acrylic resin, providing exceptional mechanical strength. The results, summarized in the accompanying table, indicate that the use of 20 wt% polysilazane achieves the optimal balance between crosslinking and minimizing foaming.

The molecular weight of all the copolymers was also analyzed to evaluate their effect on adhesive properties. The low molecular weight copolymer exhibited reduced adhesion strength ( $\sim 3.0$  MPa), attributed to insufficient molecular chain interactions and lower MMA content. In contrast, the high molecular weight copolymer demonstrated adhesion performance ( $\sim 3.7$  MPa) comparable to the standard formulation (MMA : SMA = 40% : 40%). (Fig. 2S†) However, its significantly higher viscosity posed challenges during application, leading to uneven substrate coverage. These findings highlight the critical balance between molecular weight and resin viscosity, without having to add any external solvent, in achieving optimal adhesion and application performance, with the sample used in this work.

Polysilazanes, with their backbone of  $-\text{Si}-\text{NH}-$ , react with the  $-\text{OH}$  groups of the acrylic copolymer *via* hydrolysis, forming a dense  $-\text{Si}-\text{O}-\text{Si}-$  network that is critical for providing high adhesive strength.<sup>11,38</sup> However, the final strength of the crosslinked adhesive is governed by two competing factors:

(a) the density and extent of crosslinking through the  $-\text{Si}-\text{O}-\text{Si}-$  network and (b) the formation and release of ammonia during hydrolysis. The evolution of ammonia introduces a foamy structure into the adhesive, leading to defects that reduce its overall strength. Optimizing the balance between maximizing crosslink density and minimizing foaming is crucial. Extensive experimentation revealed that a polymer-to-crosslinker weight ratio of 3 : 0.6 provides the best performance, achieving the highest tensile shear strength while minimizing defects caused by foaming.

Additionally, the molecular weight of the polymer significantly influences adhesive performance. A low molecular weight polymer lacks sufficient viscosity to remain on the substrate surface, leading to excessive penetration into porous materials like wood and inadequate interaction with polysilazanes for effective crosslinking. This also results in cohesive failure due to the inherently lower strength of the polymer. Conversely, a high molecular weight polymer exhibits excessive viscosity, hindering proper surface wetting and causing easy debonding from the substrate.

The optimal molecular weight balances these factors, ensuring adequate surface coverage and crosslinking efficiency without compromising substrate adhesion. Our polymer, with an  $M_n$  of  $2.4 \times 10^3$  g mol<sup>-1</sup>, was found to exhibit the best performance as a base material for adhesives. When combined with polysilazanes in the optimized ratio, it formed a robust adhesive system with minimal foaming and exceptional mechanical strength, leading to substrate failure rather than adhesive failure during tensile shear testing. These findings demonstrate the importance of fine-tuning both molecular weight and crosslinker ratio to achieve high-performance adhesive formulations.

The data presented in the tables above detail the tensile shear strengths of the adhesive formulations tested with both wood and aluminum substrates. Corresponding adhesive assemblies and the observed failure modes are illustrated in Fig. 7e(iv and v). From the results, it is evident that polysilazanes can serve effectively as crosslinkers in acrylic-based formulations, enabling durable and high-performance adhesive applications.

## 5 Conclusion

An acrylic-based copolymer was successfully synthesized and crosslinked using polysilazane as a crosslinker. FTIR analysis of the adhesive revealed a distinct peak corresponding to  $\text{Si}-\text{O}$ , confirming the participation of polysilazane in the crosslinking process. This reaction occurs between the  $-\text{OH}$  groups of the acrylic polymer chains and the  $-\text{Si}-\text{NH}_2$  groups of polysilazane.

The best results were achieved with an optimal polysilazane content of 20 wt%, which significantly improved the strength of the acrylic adhesive, yielding a bond strength of 4.4 MPa. This demonstrates that polysilazane is an excellent crosslinker for acrylic wood adhesives. Additionally, the same adhesive for-



mulation was tested on aluminum substrates, where it achieved a bond strength of 4.0 MPa. Overall, it can be concluded that polysilazane-crosslinked acrylic adhesives are well-suited for commercialization as a two-component adhesive system, offering ease of application and excellent strength.

## Data availability

The authors confirm that the data supporting the findings of this study are available within the article and in its supplementary materials. It will also be shared on request.

## Conflicts of interest

The authors declare no conflict of interest.

## Acknowledgements

Authors A. C., S. J., S. S., and K. D. would like to extend their gratitude to the Ministry of Education, Government of India, for providing the fellowship that enabled their research. This work has been funded by M/S SBL Specialty Coatings Private Limited, India (Grant No. SBL-2294-PPE)

## References

- 1 P. C. Briggs and G. L. Jialanella, Advances in Acrylic Structural Adhesives, *Adv. Struct. Adhes. Bonding*, 2010, 132–150, DOI: [10.1533/9781845698058.1.132](https://doi.org/10.1533/9781845698058.1.132).
- 2 C. Cui and W. Liu, Recent Advances in Wet Adhesives: Adhesion Mechanism, Design Principle and Applications, *Prog. Polym. Sci.*, 2021, **116**, 101388, DOI: [10.1016/J.PROGPOLYMSCI.2021.101388](https://doi.org/10.1016/J.PROGPOLYMSCI.2021.101388).
- 3 D. A. Aronovich and L. B. Boinovich, Structural Acrylic Adhesives: A Critical Review, *Rev. Adhes. Adhes.*, 2021, **9**(1), 65–122, DOI: [10.7569/RAA.2021.097304](https://doi.org/10.7569/RAA.2021.097304).
- 4 S. B. Lin, L. D. Durfee, R. A. Ekeland, J. McVie and G. K. Schalau, Recent Advances in Silicone Pressure-Sensitive Adhesives, *J. Adhes. Sci. Technol.*, 2007, **21**(7), 605–623, DOI: [10.1163/156856107781192274](https://doi.org/10.1163/156856107781192274).
- 5 C. Gouri, C. P. Reghunadhan Nair and R. Ramaswamy, Thermosetting Film Adhesives Based on Maleimide-Modified-Phenol-Functional Acrylic Copolymers, *J. Adhes. Sci. Technol.*, 2001, **15**(6), 703–726, DOI: [10.1163/156856101750430440](https://doi.org/10.1163/156856101750430440).
- 6 J. S. Jung, J. H. Kim, M. S. Kim, H. M. Jeong, Y. S. Kim, T. K. Kim, J. M. Hwang, S. Y. Lee and Y. L. Cho, Properties of Reactive Hot Melt Polyurethane Adhesives with Acrylic Polymer or Macromonomer Modifications, *J. Appl. Polym. Sci.*, 2008, **109**(3), 1757–1763, DOI: [10.1002/app.28291](https://doi.org/10.1002/app.28291).
- 7 Z. Czech, Crosslinking of Pressure Sensitive Adhesive Based on Water-Borne Acrylate, *Polym. Int.*, 2003, **52**(3), 347–357, DOI: [10.1002/PL.1151](https://doi.org/10.1002/PL.1151).
- 8 H. S. Joo, Y. J. Park, H. S. Do, H. J. Kim, S. Y. Song and K. Y. Choi, The Curing Performance of UV-Curable Semi-Interpenetrating Polymer Network Structured Acrylic Pressure-Sensitive Adhesives, *J. Adhes. Sci. Technol.*, 2007, **21**(7), 575–588, DOI: [10.1163/156856107781192346](https://doi.org/10.1163/156856107781192346).
- 9 H. Luo, Y. Yin, Y. Wang, Q. Li, A. Tang and Y. Liu, Enhanced Properties of a Soybean Adhesive by Modification with a Cycloaliphatic Epoxy Resin, *Int. J. Adhes. Adhes.*, 2022, **114**, 103026, DOI: [10.1016/J.IJADHADH.2021.103026](https://doi.org/10.1016/J.IJADHADH.2021.103026).
- 10 J. Hong, Y. Kwon, M. S. Kwon and C. Cha, Aziridine-Capped Poly(Ethylene Glycol) Brush Copolymers with Tunable Architecture as Versatile Cross-Linkers for Adhesives, *ACS Appl. Polym. Mater.*, 2022, **4**(3), 2105–2115, DOI: [10.1021/ACSAPM.1C01894/ASSET/IMAGES/LARGE/AP1C01894\\_0010.JPG](https://doi.org/10.1021/ACSAPM.1C01894/ASSET/IMAGES/LARGE/AP1C01894_0010.JPG).
- 11 H. W. Park, J. W. Park, J. H. Lee, H. J. Kim and S. Shin, Property Modification of a Silicone Acrylic Pressure-Sensitive Adhesive with Oligomeric Silicone Urethane Methacrylate, *Eur. Polym. J.*, 2019, **112**, 320–327, DOI: [10.1016/J.EURPOLYMJ.2019.01.021](https://doi.org/10.1016/J.EURPOLYMJ.2019.01.021).
- 12 A. Gomez-Lopez, B. Grignard, I. Calvo, C. Detrembleur and H. Sardon, Synergetic Effect of Dopamine and Alkoxy silanes in Sustainable Non-Isocyanate Polyurethane Adhesives, *Macromol. Rapid Commun.*, 2021, **42**(3), 2000538, DOI: [10.1002/marc.202000538](https://doi.org/10.1002/marc.202000538).
- 13 J. Ma, S. Zhou, Y. Wang, R. Chen, S. Wang, F. Zhang and Y. P. He, Preparation and Properties of Vinyltriethoxysilane-Modified Waterborne Acrylate Resins, *Polymer*, 2024, **314**, 127781, DOI: [10.1016/J.POLYMER.2024.127781](https://doi.org/10.1016/J.POLYMER.2024.127781).
- 14 S. Sen, A. Chatterjee, D. Ramakanth, S. Singh and P. K. Maji, Recent Advances in Cathodic Electrodeposition Coatings with Special Reference to Resin Materials: A Comprehensive Review, *Prog. Org. Coat.*, 2024, **190**, 108387, DOI: [10.1016/J.PORGCOAT.2024.108387](https://doi.org/10.1016/J.PORGCOAT.2024.108387).
- 15 H. W. Park, H. S. Seo, K. Kwon and S. Shin, Preparation of UV-Curable PSAs by Grafting Isocyanate-Terminated Photoreactive Monomers and the Effect of the Functionality of Grafted Monomers on the Debonding Properties on Si Wafers, *RSC Adv.*, 2023, **13**(17), 11874–11882, DOI: [10.1039/d3ra00398a](https://doi.org/10.1039/d3ra00398a).
- 16 J. S. Andre, J. Grant, E. Greyson, X. Chen, C. Tucker, R. Drumright, C. Mohler and Z. Chen, Molecular Interactions between Amino Silane Adhesion Promoter and Acrylic Polymer Adhesive at Buried Silica Interfaces, *Langmuir*, 2022, **38**(19), 6180–6190, DOI: [10.1021/ACS.LANGMUIR.2C00602/ASSET/IMAGES/LARGE/LA2C00602\\_0010.JPG](https://doi.org/10.1021/ACS.LANGMUIR.2C00602/ASSET/IMAGES/LARGE/LA2C00602_0010.JPG).
- 17 H. W. Park, H. S. Seo, J. H. Lee and S. Shin, Adhesion Improvement of the Acrylic Pressure-Sensitive Adhesive to Low-Surface-Energy Substrates Using Silicone Urethane Dimethacrylates, *Eur. Polym. J.*, 2020, **137**, 109949, DOI: [10.1016/J.EURPOLYMJ.2020.109949](https://doi.org/10.1016/J.EURPOLYMJ.2020.109949).
- 18 Z. Pan and L. Zhu, Synthesis of a Siloxane Oligomer Containing Methyl Acryloxy Group for Promoting the Adhesion of Addition-Type Silicone Rubber to Copper Plate, *Int. J. Adhes. Adhes.*, 2023, **123**, 103355, DOI: [10.1016/J.IJADHADH.2023.103355](https://doi.org/10.1016/J.IJADHADH.2023.103355).



19 M. Günthner, K. Wang, R. K. Bordia and G. Motz, Conversion Behaviour and Resulting Mechanical Properties of Polysilazane-Based Coatings, *J. Eur. Ceram. Soc.*, 2012, **32**(9), 1883–1892, DOI: [10.1016/J.JEURCERAMSOC.2011.09.005](https://doi.org/10.1016/J.JEURCERAMSOC.2011.09.005).

20 A. Chatterjee, S. Sen, S. Singh, S. Bhardwaj and P. K. Maji, Corrosion Protection of Mild Steel via Cerium Nitrate Loaded Acrylic-Vinyl Polysilazane Based Hybrid Coatings, *Prog. Org. Coat.*, 2024, **197**, 108831, DOI: [10.1016/J.PORGCOAT.2024.108831](https://doi.org/10.1016/J.PORGCOAT.2024.108831).

21 Y. Zhan, W. Li, R. Grottenmüller, C. Minnert, T. Krasemann, Q. Wen and R. Riedel, Rapid Curing of Polysilazane Coatings at Room Temperature via Chloride-Catalyzed Hydrolysis/Condensation Reactions, *Prog. Org. Coat.*, 2022, **167**, 106872, DOI: [10.1016/J.PORGCOAT.2022.106872](https://doi.org/10.1016/J.PORGCOAT.2022.106872).

22 Y. Zhan, R. Grottenmüller, W. Li, F. Javaid and R. Riedel, Evaluation of Mechanical Properties and Hydrophobicity of Room-Temperature, Moisture-Curable Polysilazane Coatings, *J. Appl. Polym. Sci.*, 2021, **138**(21), 50469, DOI: [10.1002/app.50469](https://doi.org/10.1002/app.50469).

23 Widyastuti, S. Hardiyanti, W. S. Muhaqqi Al Haq, L. L. Zulfa, N. Safrida, A. N. Hakim, L. Mariani, H. Purnomo, Sulistijono and R. A. Wahyuono, Morphological and Mechanical Studies of  $\text{Al}_2\text{O}_3 - \text{Na}_2\text{SiO}_3$  as a Skin Barrier Coated with  $\text{TiO}_2$  for Carbon Fiber Reinforced Composite Materials, *RSC Adv.*, 2024, **14**(14), 9483–9496, DOI: [10.1039/D3RA08518J](https://doi.org/10.1039/D3RA08518J).

24 N. Widyastuti, L. L. Zulfa, W. A. Rizaldi, J. Azhar, N. Safrida, A. D. Pratama, R. A. Wahyuono, N. Sulistijono, R. Fajarin and A. N. Hakim, A Study on Thermal Behaviour of Thermal Barrier Coating: Investigation of Particle Size, YSZ/Polysilazane, Time and Temperature Curing Effect, *RSC Adv.*, 2024, **14**(34), 24687–24702, DOI: [10.1039/D4RA03620D](https://doi.org/10.1039/D4RA03620D).

25 J. Xue, L. Zhang, Y. Hou, D. Wang, L. Li and G. Wen, Polysilazane-Based High-Temperature Adhesives for the Joints of Amorphous SiBON Ceramic Composites, *J. Manuf. Process.*, 2023, **88**, 220–231, DOI: [10.1016/J.JMAPRO.2023.01.016](https://doi.org/10.1016/J.JMAPRO.2023.01.016).

26 C. Ma, H. Pang, Y. Shen, Z. Liang, J. Li, S. Zhang and J. Shi, Plant Polyphenol-Inspired Crosslinking Strategy toward High Bonding Strength and Mildew Resistance for Soy Protein Adhesives, *Macromol. Mater. Eng.*, 2021, **306**(12), 2100543, DOI: [10.1002/MAME.202100543](https://doi.org/10.1002/MAME.202100543).

27 D. Maity, R. Tade and A. S. Sabinis, Development of Bio-Based Polyester-Urethane-Acrylate (PUA) from Citric Acid for UV-Curable Coatings, *J. Coat. Technol. Res.*, 2023, **20**(3), 1083–1097, DOI: [10.1007/S11998-022-00728-5/TABLES/7](https://doi.org/10.1007/S11998-022-00728-5/TABLES/7).

28 B. Gardelle, S. Duquesne, C. Vu and S. Bourbigot, Thermal Degradation and Fire Performance of Polysilazane-Based Coatings, *Thermochim. Acta*, 2011, **519**(1–2), 28–37, DOI: [10.1016/J.TCA.2011.02.025](https://doi.org/10.1016/J.TCA.2011.02.025).

29 A. H. Moradifard, A. Hassani Joshaghani, H. Mazaheri, M. Salimi and K. Faghihi, Preparation and Evaluation of Adhesion and Wettability Properties of Acetate–Acrylate–Siloxane Adhesive, *Polym. Bull.*, 2024, **81**(4), 3583–3597, DOI: [10.1007/s00289-023-04878-3](https://doi.org/10.1007/s00289-023-04878-3).

30 R. V. Gadhave, P. A. Mahanwar and P. T. Gadekar, Cross-Linking of Polyvinyl Alcohol/Starch Blends by Epoxy Silane for Improvement in Thermal and Mechanical Properties, *BioResources*, 2019, **14**(2), 3833–3843.

31 J. R. Gouveia, R. R. de Sousa Júnior, A. O. Ribeiro, S. A. Saraiva and D. J. dos Santos, Effect of Soft Segment Molecular Weight and NCO:OH Ratio on Thermomechanical Properties of Lignin-Based Thermoplastic Polyurethane Adhesive, *Eur. Polym. J.*, 2020, **131**, 109690, DOI: [10.1016/J.EURPOLYMJ.2020.109690](https://doi.org/10.1016/J.EURPOLYMJ.2020.109690).

32 A. Chatterjee, S. Sen, S. Bhardwaj and P. K. Maji, Polysilazane-Cross-Linked Acrylic Coatings for Wood: A Versatile Solution for Weather Resistance, Stain Repellence, and Fire Safety, *ACS Appl. Eng. Mater.*, 2025, **3**(2), 502–512, DOI: [10.1021/ACSAENM.4C00803](https://doi.org/10.1021/ACSAENM.4C00803).

33 T. Todorovic, E. Norström, F. Khabbaz, J. Brücher, E. Malmström and L. Fogelström, A Fully Bio-Based Wood Adhesive Valorising Hemicellulose-Rich SideStreams from the Pulp Industry, *Green Chem.*, 2021, **23**(9), 3322–3333, DOI: [10.1039/D0GC04273K](https://doi.org/10.1039/D0GC04273K).

34 M. Bartkowiak, Z. Czech, K. Mozelewska and M. Nowak, Influence of Thermal Reactive Crosslinking Agents on the Tack, Peel Adhesion, and Shear Strength of Acrylic Pressure-Sensitive Adhesives, *Polym. Test.*, 2020, **90**, 106603, DOI: [10.1016/J.POLYMERTESTING.2020.106603](https://doi.org/10.1016/J.POLYMERTESTING.2020.106603).

35 W. Liu, Y. Luo and C. Xu, A New Organosilicon Adhesive Based on Polysiloxane and Polysilazane, *High Perform. Polym.*, 2013, **25**(5), 543–550, DOI: [10.1177/0954008312473763](https://doi.org/10.1177/0954008312473763).

36 *Polysilazanes for Coating Applications—Welcome to DTU Research Database.* <https://orbit.dtu.dk/en/publications/polysilazanes-for-coating-applications> (accessed 2024-09-14).

37 R. Sønderbæk-Jørgensen, S. Meier, K. Dam-Johansen, A. L. Skov and A. E. Daugaard, Reactivity of Polysilazanes Allows Catalyst-Free Curing of Silicones, *Macromol. Mater. Eng.*, 2022, **307**(9), 2200157, DOI: [10.1002/MAME.202200157](https://doi.org/10.1002/MAME.202200157).

38 M. Saleh, A. Bhuiyan, K. Wang, F. Razaviamri and B. P. Lee, Salicylhydroxamic Acid Containing Structural Adhesive, *RSC Appl. Polym.*, 2024, **2**(5), 838–846, DOI: [10.1039/D4LP00139G](https://doi.org/10.1039/D4LP00139G).

